Spatio-temporal variability of the carbonate system and air-sea CO2 fluxes in the South Yellow Sea and East China Sea during the warm seasons

Chun-Ying Liu[1], Xue Deng[2], Gui-Ling Zhang[2], Ming Xin[3], and Wei-Jun Cai[1]

[1]University of Delaware
[2]Ocean University of China
[3]the First Institute of Oceanography

November 24, 2022

Posted on 24 Nov 2022 — CC-BY-NC 4 — https://doi.org/10.1002/essoar.10502680.1 — This a preprint and has not been peer reviewed. Data may be preliminary.

Abstract

Due to the complex physical and biogeochemical conditions, the adjacent South Yellow Sea (SYS) and East China Sea (ECS) are ideal sites for studying different carbonate characteristics in marginal seas. The distributions of carbonate system parameters were investigated in this region in early spring and summer. Overall, dissolved inorganic carbon (DIC) and alkalinity concentrations in the SYS were higher than those in the ECS due to the Yellow River runoff which was featured with intensive carbonate weathering and erosion. Low DIC, alkalinity and high pH values were observed in the Zhe-Min Coastal Current with intensive primary production in spring caused by the Changjiang River and Taiwan Warm Current. Temperature and biological activities were the primary drivers in controlling the partial pressure of CO2 (pCO2) variability in the SYS, whereas temperature was the only dominant factor in the outer shelf of the ECS, which was heavily impacted by the Kuroshio Current. The pCO2 dynamics was controlled by primary production and physical mixing in the Changjiang River plume and the inner and middle shelves of the ECS, due to the influence of the Changjiang River with high nutrient supply. Overall, strong CO2 sinks (-4.11 $\pm$ 5.28 mmol m-2d-1) turned into weak sources (0.88 $\pm$ 5.09 mmol m-2d-1) in the entire study area from spring to summer. Specifically, the SYS and ECS offshore waters changed from CO2 sinks in spring to sources in summer, while the Changjiang River plume always served as a CO2 sink.

Spatio-temporal variability of the carbonate system and air-sea CO_2 fluxes in the South Yellow Sea and East China Sea during the warm seasons

Xue Deng[1,2], Gui-Ling Zhang[1,2], Ming Xin[2,3], Chun-Ying Liu[1,2,*], Wei-Jun Cai[4]

[1] Key Laboratory of Marine Chemistry Theory and Technology, Ministry of Education, Qingdao 266100, PR China

[2] Laboratory for Marine Ecology and Environmental Science, Qingdao National Laboratory for Marine Science and Technology, Qingdao 266071, PR China

[3] Key Laboratory for Marine Bioactive Substances and Modern Analytical Technology, the First Institute of Oceanography, Ministry of Natural Resources, Qingdao 266061, PR China

[4] School of Marine Science and Policy, University of Delaware, Newark, DE 19716, United States

*Corresponding author: roseliu@ouc.edu.cn

Key Points:

- Strong CO_2 sinks turned into weak sources in the entire study area from spring to summer

- The study area was divided into three subregions to separately examine the driver mechanisms of the pCO_2 variations
- The pCO_2 variability was controlled by the combined influences of temperature, biological activity and physical mixing

Abstract

Due to the complex physical and biogeochemical conditions, the adjacent South Yellow Sea (SYS) and East China Sea (ECS) are ideal sites for studying different carbonate characteristics in marginal seas. The distributions of carbonate system parameters were investigated in this region in early spring and summer. Overall, dissolved inorganic carbon (DIC) and alkalinity concentrations in the SYS were higher than those in the ECS due to the Yellow River runoff which was featured with intensive carbonate weathering and erosion. Low DIC, alkalinity and high pH values were observed in the Zhe-Min Coastal Current with intensive primary production in spring caused by the Changjiang River and Taiwan Warm Current. Temperature and biological activities were the primary drivers in controlling the partial pressure of CO_2 (pCO_2) variability in the SYS, whereas temperature was the only dominant factor in the outer shelf of the ECS, which was heavily impacted by the Kuroshio Current. The pCO_2 dynamics was controlled by primary production and physical mixing in the Changjiang River plume and the inner and middle shelves of the ECS, due to the influence of the Changjiang River with high nutrient supply. Overall, strong CO_2 sinks (-4.11 ± 5.28 mmol $m^{-2}d^{-1}$) turned into weak sources (0.88 ± 5.09 mmol $m^{-2}d^{-1}$)

in the entire study area from spring to summer. Specifically, the SYS and ECS offshore waters changed from CO_2 sinks in spring to sources in summer, while the Changjiang River plume always served as a CO_2 sink.

Keywords: Carbon cycle, air-sea CO_2 flux, the South Yellow Sea and East China Sea, seasonal variations

Plain Language Summary

Although the South Yellow Sea (SYS) and East China Sea (ECS) are adjacent to each other, the biogeochemical characteristics of them are very different. Therefore, a study of the SYS and ECS together will allow us a better understanding of the processes determining the spatial and temporal variations of the carbonate system in continental seas, which is an important step toward estimating global air-sea CO_2 fluxes. In this study, two cruises were conducted in early spring and summer to investigate the distributions of the carbonate system in the SYS and ECS. High dissolved inorganic carbon (DIC) and alkalinity were observed in the SYS under the influence of Yellow River with high DIC and alkalinity discharges. However, low DIC, alkalinity and high pH values occurred in the Zhe-Min Coastal Current. The distribution and variability of the partial pressure of CO_2 were associated with temperature, biological activity and physical mixing. Under the combined impacts of the above factors, the SYS and ECS offshore waters changed from CO_2 sinks in spring to sources in summer, while the Changjiang River plume always served as a

CO_2 sink. Overall, Strong CO_2 sinks turned into weak sources in this region from spring to summer.

1 Introduction

In the last two decades, continental shelves have drawn increasing attention in the global ocean carbon cycle research due to the fact that they provide 15–30% of the oceanic primary production and represent 50% of ocean organic carbon burial in sediments, although shelves just comprising approximately 7% of the world's ocean surface area (Bauer et al., 2013; Borges et al., 2005; Cai, 2011; Chen, 2003). The continental shelves are distinguished by the intense physical, chemical and biological processes, and considered to be significant contributors to the global carbon cycle (Mackenzie et al., 1991). It is therefore necessary to understand and accurately account for the variability of air-sea CO_2 flux and carbonate chemistry of continental shelves although it remains a tremendous challenge to make satisfactory progresses (Bauer et al., 2013; Zhai et al., 2014).

There are large spatial and temporal variations in surface seawater biogeochemistry and air-sea CO_2 exchanges across heterogeneous continental shelves (Takahashi et al., 2009). An ocean margin province-based synthesis by Cai et al. (2006) suggested that continental marginal seas at low latitudes were the major CO_2 sources (Cai et al., 2003, 2004; Goyet et al., 1998), but those in mid-high latitudes were the sinks of atmospheric CO_2 (DeGrandpre et al., 2002; Thomas et al., 2005; Tsunogai et al., 1999). Recently, Dai et al. (2013) suggested that margins receiving river inputs (RiOMar) were largely a CO_2 sink while those receiving ocean inputs (OceMar) were largely sources of CO_2 to the atmosphere. However, these broad classifications may oversimplify the field observations and the mechanisms leading to these synthesis statements require further supports from many field studies in dissimilar margins. For example, the North Sea, a European continental shelf sea, is a CO_2 sink in the northern part but a CO_2 source in the southern part under the influence of temperature, terrestrial inputs and biological activity from north to south (Bozec et al., 2005; Kempe & Pegler, 1991; Omar et al., 2010; Thomas et al., 2005). Similarly, the partial pressure of CO_2 (pCO_2) distribution also shows a different spatial trend in the adjacent South Yellow Sea (SYS) and East China Sea (ECS), resulting from different topography, ocean circulation and biogeochemical conditions. In the north, the SYS, as a semi-enclosed marginal sea, is a net annual CO_2 source because of its long water residence time and limited water exchange with open ocean (Qu et al., 2014; Xue et al., 2011; Zhang et al., 2010). In contrast, in the south, the ECS is an eminent continental shelf pump for efficient transferring atmospheric CO_2 to the deep sea and serves as an annual net sink of atmospheric CO_2 (Song et al., 2018; Tsunogai et al., 1999; Wang et al., 2000; Zhai & Dai, 2009). Therefore, the carbonate characteristics of these two seas are different. However, the previous studies tend to study their air-sea flux separately, even if the SYS and ECS are adjacent to each other. To our best knowledge, the carbonate system of the entire SYS and ECS (together called the South Yellow-East China Sea region) has only been investigated in the spring and summer of 2011 and the summer of 2013 (Qu et al., 2015, 2017) to date.

With those limited studies, the spatial resolution of pCO_2 distributions is still lacking because the pCO_2 in Qu et al. (2015, 2017) was calculated by CO2SYS based on the discrete pH and total alkalinity (TA) instead of continuous underway measurement, and the air-sea CO_2 flux based on discrete estimations also had great uncertainties.

A better understanding of spatial and temporal variations of carbonate system in the South Yellow-East China Sea region is important to merge its CO_2 flux into the global carbon cycle. Therefore, in this study, we investigated high spatial resolutions of discrete pH, dissolved inorganic carbon (DIC) and TA samples as well as underway pCO_2 in the South Yellow-East China Sea region with intensive biological activity based on two cruises from 27 March to 11 April, 2017 and 27 June to 17 July, 2018. We also calculated the air-sea CO_2 fluxes and examined the driver mechanisms to impact the pCO_2 variations and air-sea CO_2 fluxes. This study fills in the knowledge gap by not only providing an updated dataset on the air-sea CO_2 fluxes in the South Yellow-East China Sea region, but also improving our understanding of carbon cycles in continental seas.

2 Materials and Methods

2.1 Study area

The South Yellow and East China Sea, which is located in the northwestern Pacific Ocean between 26–37°N and 119–125°E (Figure 1). The SYS is a semi-enclosed marginal sea, which is surrounded by the Shandong and Korean Peninsulas and bordered on the north by the North Yellow Sea and on the south by the ECS. It is distinguished and dominated by several major water masses in different seasons, including the Yellow Sea Warm Current, Yellow Sea Cold Water Mass, coastal water currents along both the Chinese and Korean coasts and Changjiang River (Figure 1). Moreover, the Subei Shoal waters in the southwestern SYS, being one of the most turbid coasts in China, load numerous sediments into the SYS annually (Wang et al., 2011a). Hence, the SYS is strongly influenced by nearshore biogeochemical processes, intense anthropogenic activities to a great extent and is isolated from open sea (Choi et al., 2019). However, the ECS is located to the south of the SYS and the western three quarters of the ECS is occupied by the continental shelf, while the eastern part is deep and opens to the Pacific Ocean (Chen, 2009). The materials from the Pacific Ocean is easily exchanged with the ECS by the Kuroshio Current (KC) and Taiwan Warm Current (TWC), while the Changjiang River brings large amounts of terrigenous nutrients into the ECS (Qu et al., 2017). Thus, the carbonate system in the ECS is strongly subjected to the continental shelf pump between the nearshore and open sea (Tsunagai et al., 1999). Given these points, the South Yellow-East China Sea region becomes a biogeochemical hotspot all the time due to the large differences in the physical and biogeochemical conditions between the SYS and ECS.

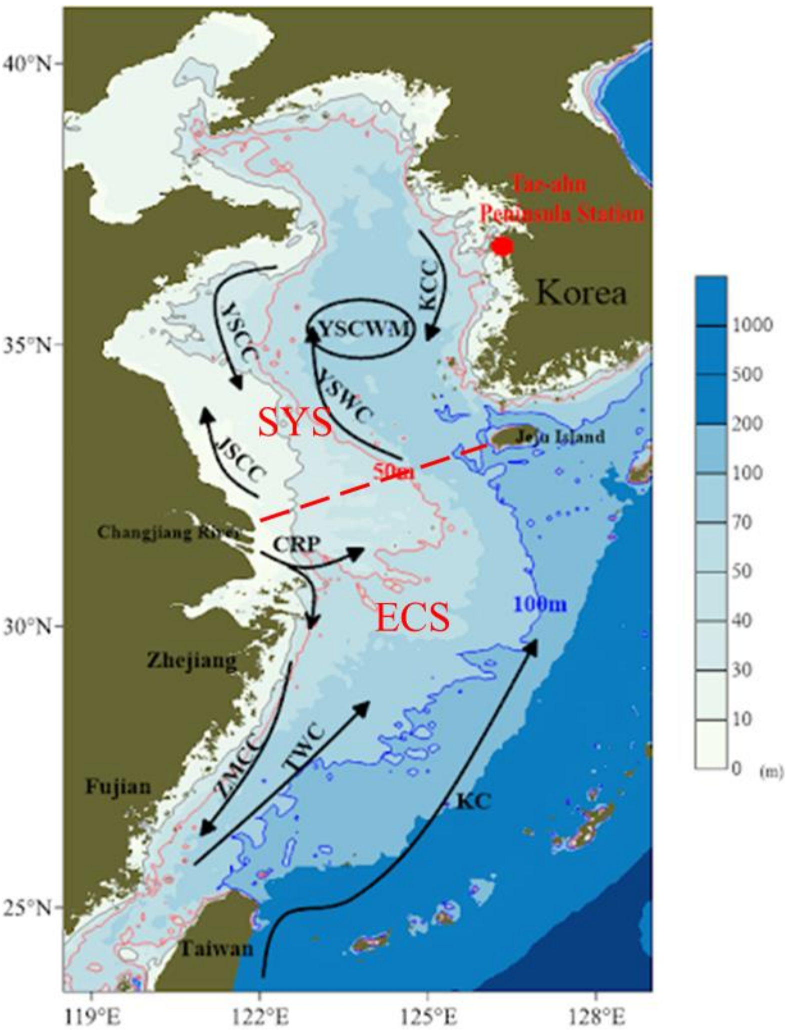

Figure 1. Topography and schematic map of the current system in the study area. The boundary of the South Yellow Sea (SYS) and East China Sea (ECS) is indicated by the red dashed-line. The currents described as arrows include the Yellow Sea Coastal Current (YSCC), Yellow Sea Warm Current (YSWC), Yellow Sea Cold Water Mass (YSCWM), Korea Coastal Current (KCC), Jiangsu Coastal Current (JSCC), Changjiang River plume (CRP), Zhe-Min Coastal Current (ZMCC), Taiwan Warm Current (TWC) and Kuroshio Current (KC) (Chen, 2009). The red and blue solid lines on the continental shelf are the depth contour of 50 and 100 m, respectively. The red dot (126.133°E, 36.738°N) in the west part of South Korea is the Tae-ahn Peninsula Station (https://www.esrl.noaa.gov).

2.2 Sampling

Two cruises were carried out aboard the R/V *"Dongfanghong II"* from 27 March to 11 April, 2017 and 27 June to 17 July, 2018 to represent the early spring and summer, respectively. The study area and sampling stations are shown in Figure 2.

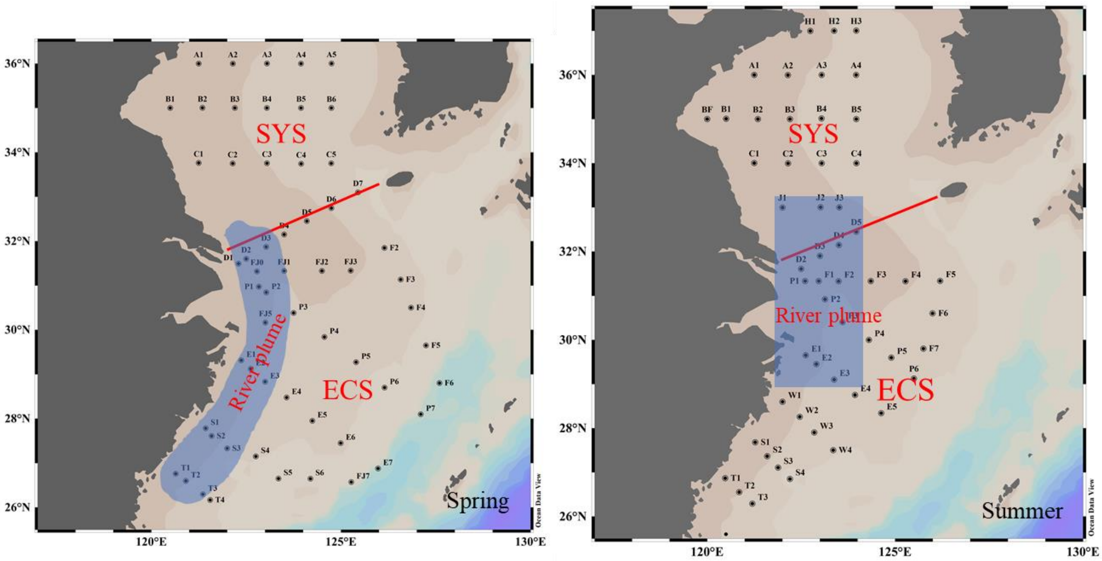

Figure 2. Sampling stations of 2017 spring (left) and 2018 summer (right) cruises. The blue shadows represent the Changjiang River plume; the South Yellow Sea (SYS) and East China Sea (ECS) are divided by the red solid line.

Water samples were collected using 12 L Niskin bottles mounted onto a Seabird 911-plus Conductivity-Temperature-Depth system (CTD, SeaBird Inc. Bellevue, WA, USA), which was used to measure the temperature and salinity of water column. DO samples were collected, fixed and analyzed on board as described by the classic Winkler procedure (Dickson, 1994). pH was collected into a 100 mL narrow-mouth glass bottle and kept in a thermal bath (25 ± 0.1 °C) for 30–60 min before determination. DIC and TA samples were stored in 250 mL borosilicate glass bottles and overflowed at least twice their volume to minimize contact with air, then poisoned with 100 μL of saturated $HgCl_2$ immediately, sealed and preserved at room temperature until determination (Huang et al., 2012). 300 mL water samples were filtered through a 0.7 μm-pore Whatman glass fiber filter (GF/F, pre-combusted at 400 °C for 4 h), and materials collected on the membrane were preserved at -20 °C and used for analyzing Chlorophyll *a* (Chl *a*).

To monitor levels of $p\mathrm{CO_2}$, surface water was continuously pumped from 1–2 m below the sea level through an underway $p\mathrm{CO_2}$ analyzer (AS-P2, Apollo SciTech Inc., USA) with a Picarro detector (G2301, Picarro Inc., USA) installed in the shipboard laboratory. Briefly, surface water was pumped to the main shower-head equilibrator at a rate of 2.5 L min^{-1} to get rapid gas exchange. After the sample was equilibrated, the well-mixed gas first passed through the water condenser and desiccant, which removed most of the water vapor, and then the equilibrated gas was delivered to the detector (Picarro G2301). The detector was calibrated every 9 h against three CO_2 gas standards (0, 198 and 403 ppm), which were provided by Beijing Certified Reference Material Center. Some values of $x\mathrm{CO_2}$ outside of the concentration range of the standard gases were also used in this study because the biases caused by the out-of-range values are generally subtle (Pierrot et al., 2009). The uncertainty of $x\mathrm{CO_2}$ measurements was less than 50 ppbv over 5 min internals (Li et al., 2017).

2.3 Analytical methods

pH was measured onboard at 25 ± 0.1 °C by Fisher pH meter (Star A211) combining with a Ross Orion combination electrode (Ross-8102) on a National Bureau of Standards (NBS) scale with a precision of ± 0.01 units. pH values were corrected to the in-situ temperature using CO2SYS. 1 mL of each DIC sample was acidified by 10% phosphoric acid, then the extracted CO_2 gas with carrier gas was quantified via an infrared gas analyzer (AS-C3, Apollo SciTech Inc., USA) as described in Cai et al. (2004). TA samples were determined by Gran titration on a 25 mL sample volume using the open-cell method with a semi-automatic potentiometric titration system (AS-ALK2, Apollo SciTech Inc., USA) (Cai et al., 2010). Both DIC and TA measurements were calibrated against certified reference materials from A. G. Dickson's lab at Scripps Institute of Oceanography (Batches #162 and #171) at a precision of ± 2 μmol kg^{-1} (Huang et al., 2012).

Chl *a* on the membrane was extracted in 90% acetone and then analyzed by a fluorescence spectrophotometer (F-4500, Hitachi, Japan) based on the procedure described by Parsons et al. (1984).

2.4 Air-sea CO_2 flux estimation

In this study, the pCO_2 at the temperature of equilibration ($pCO_2(eq)$, unit: μatm) in equation (1) is calculated as following and then the pCO_2 at the in-situ temperature ($pCO_2(water)$, unit: μatm) in equation (2) is calculated by the expression of Takahashi et al. (1993):

$$pCO_2(eq) = xCO_2 \times [P_b(eq) - P_w(eq)] \quad (1)$$

$$pCO_2(water) = pCO_2(eq) \times \exp[0.0423 \times (SST - T_{eq})] \quad (2)$$

where xCO_2 is the CO_2 mole fraction concentration of the seawater CO_2 in the dried sample gas flow (ppm), P_b(eq) is the barometric pressure of equilibration and P_w(eq) is the water vapor pressure at 100% humidity calculated by the equilibrated temperature (T_{eq}, °C) and in-situ salinity (Weiss & Price, 1980). *SST* (°C) is the in-situ temperature of surface water, the temperature difference between the in-situ water and the equilibration was less than 0.5 °C.

The air-sea CO_2 fluxes (FCO_2, mmol m^{-2} d^{-1}) were estimated as follows:

$$FCO_2 = 0.24 \times k \times K_H \times [pCO_2(water) - pCO_2(air)] \quad (3)$$

where k (cm h^{-1}) is the gas transfer velocity of CO_2, K_H (mol L^{-1} atm^{-1}) is the solubility constant of CO_2, calculated from in-situ temperature and salinity (Weiss, 1974), and $pCO_2(water)$ and $pCO_2(air)$ are the pCO_2 in the surface seawater and the atmosphere, respectively. The atmospheric pCO_2 values (417 μatm in April 2017 and 398 μatm in July 2018) were estimated from the monthly atmospheric xCO_2 (418.49 ppm in April 2017 and 410.14 ppm in July 2018) at Tae-ahn Peninsula (126.133°E, 36.738°N, Figure1) (https://www.esrl.noaa.gov), after correction for water vapor pressure at 100% humidity with in-situ temperature and salinity data (Weiss and Price, 1980). A positive flux value represents a release of CO_2 from the water body to the atmosphere, while a negative value indicates CO_2 transfer from the atmosphere to the water body. The gas transfer coefficient was calculated from wind speed based on the Wanninkhof (2014) empirical function:

$$k\ (\text{cm h}^{-1}) = 0.251 \times U^2 \times (Sc/660)^{-0.5} \quad (4)$$

where U (m s^{-1}) is the wind speed at 10 m above the water surface, the reanalyzed monthly averaged wind speed (5.95 and 6.00 m s^{-1} in spring and summer, respectively) provided by the European Center for Medium-Range Weather Forecasts (ECMWF) was employed to calculate the air-sea CO_2 fluxes; Sc is the Schmidt number of CO_2 in seawater; 660 is the Sc value in seawater at 20 °C.

3 Results

3.1 Hydrographic conditions

Surface seawater temperature (SST) presented significant temporal and spatial variations (Figure 3). SST was in the range of 6.91–24.47 and 15.82–28.17 °C, with average (± SD) values of 14.00 ± 5.00 and 24.94 ± 2.80 °C, respectively, in the spring and summer throughout the South Yellow-East China Sea region. clearly SST increased homogeneously with the decreasing latitudes in spring and summer. On average, SST in the SYS was 7.31 and 4.94 °C colder than that in the ECS in early April and July, respectively. The temperature difference between the SYS and ECS in April was due to the increase of atmospheric temperature from north to south in the northern hemisphere, while in July, it could be mainly attributed to the intrusion of the TWC or KC with the influence of the summer monsoon (Chen, 2009). The ranges of salinity in spring (range: 25.81–34.94, average: 32.59 ± 1.89) and summer (23.63–34.14, average: 31.58 ± 2.26) were not greatly different. The main feature was that a water tongue with relatively low salinity rushed out of Changjiang estuary and formed a plume, indicating the influence of the Changjiang River on the junction of the SYS and ECS. This plume feature was stronger in summer than spring.

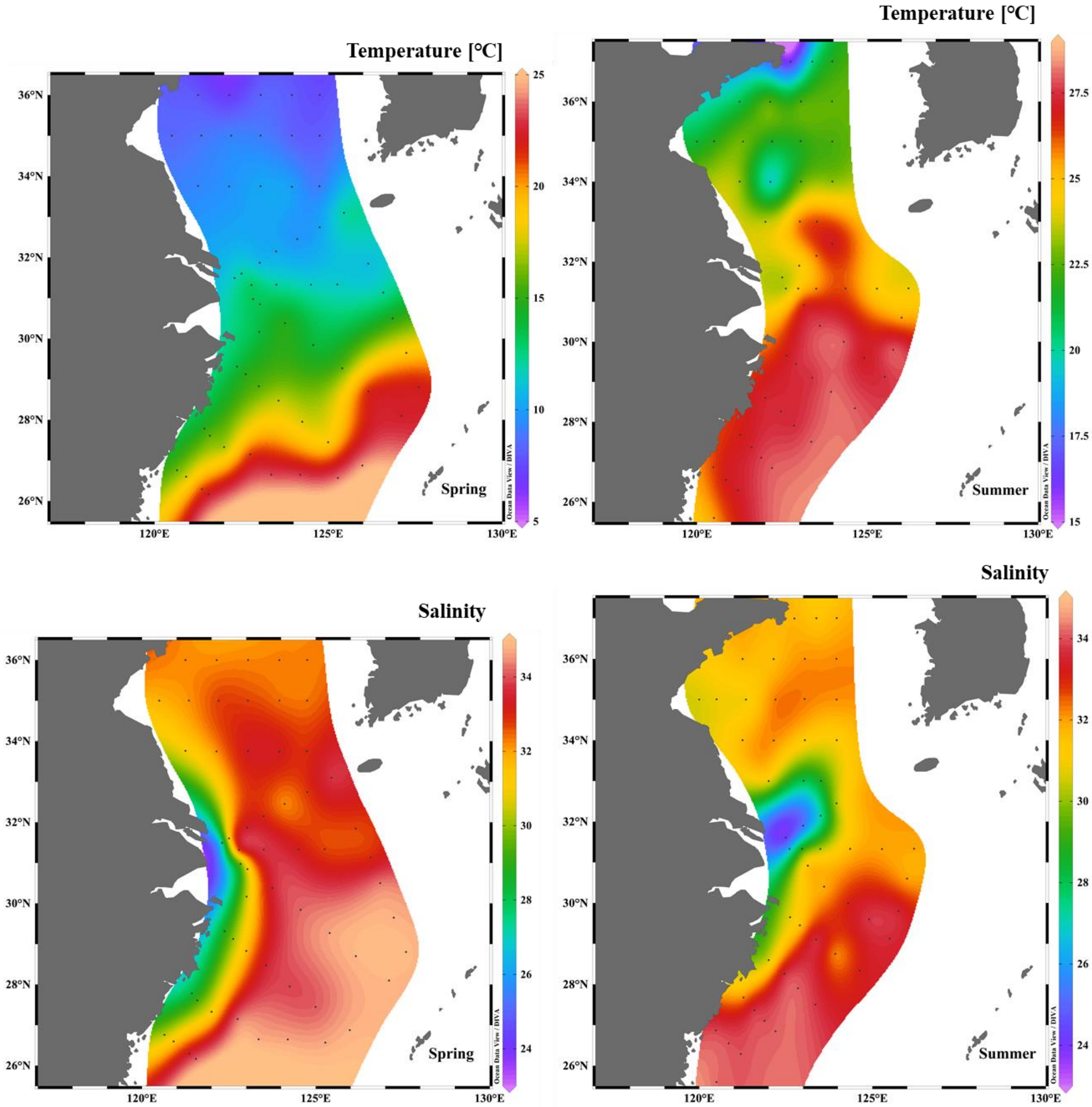

Figure 3. Horizontal distributions of temperature (°C) and salinity in the surface water of spring and summer.

From early spring to summer, the surface Chl *a* exhibited considerable variation (Figure 4). Overall, Chl *a* concentration of the SYS in early spring (0.59 ± 0.51 μg L^{-1})

was lower than that (1.00 ± 0.98 μg L^{-1}) in summer because of the weak biological activity at lower temperature. In summer, high Chl *a* value appeared in the southwestern part of the SYS, which was enhanced by the abundant nutrient inputs from the Changjiang River. In the ECS, high concentrations of surface Chl *a* (3.46–8.80 μg L^{-1}) in spring were found in the southwest part of the shelf near the coast. Also noted was high Chl *a* concentration in the northwest part of the ECS in summer, which was also due to the large amount of nutrients loading from the Changjiang River. In contrast, low surface Chl *a* (< 0.50 μg L^{-1}) was observed in the middle and outer shelves of the ECS in both spring and summer.

O_2 saturation in surface water were oversaturated conditions albeit with a few exceptions (Figure 4). The average O_2 saturations were 109 ± 13 and 152 ± 17% in the surface layer of the South Yellow-East China Sea region during spring and summer cruises, respectively. Thus, O_2 saturation in the surface layer of summer was higher than that in spring, due to the growth of phytoplankton and water stratification, which limited the exchanges between high DO in the surface layer and low DO in the bottom layer.

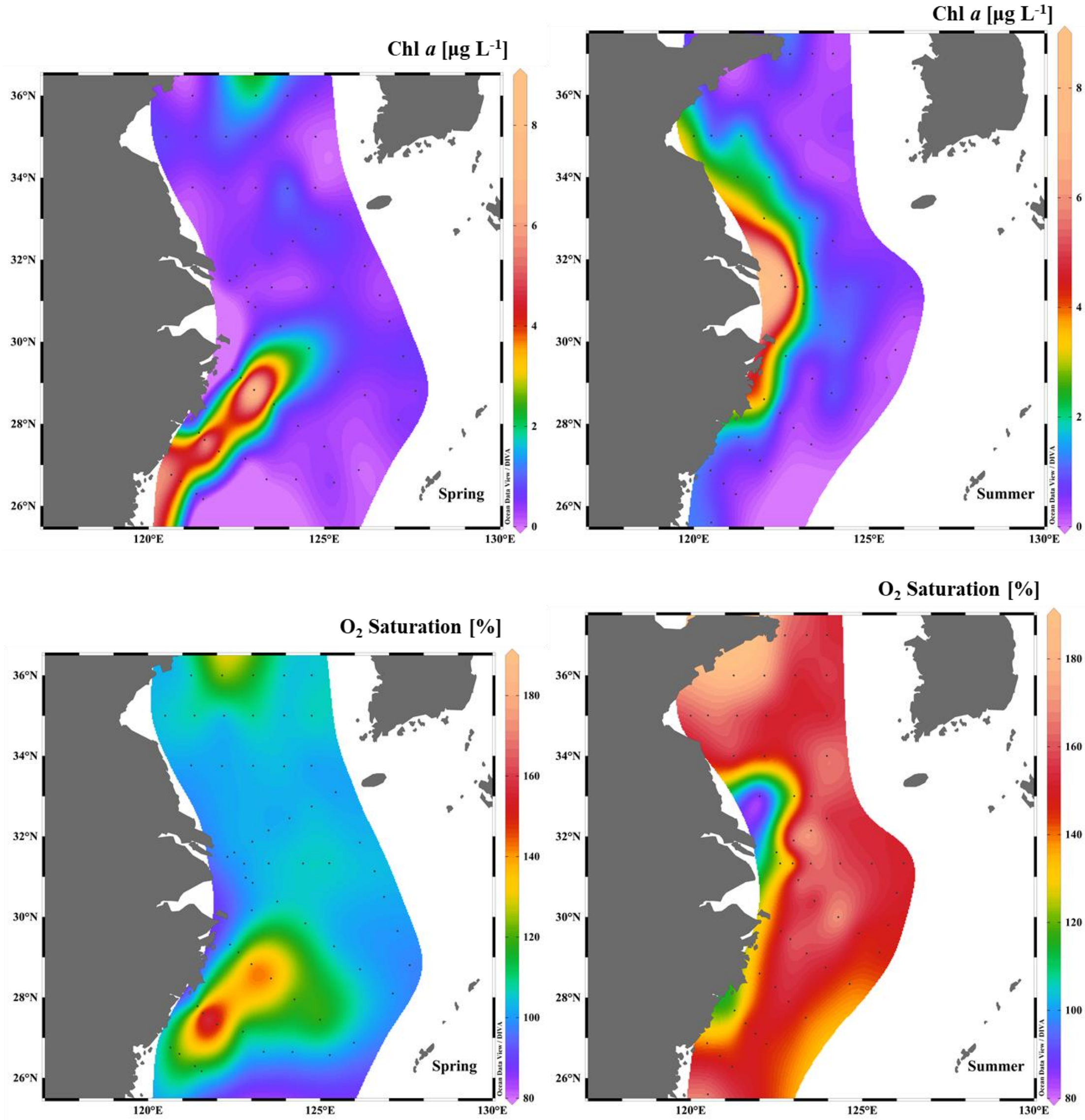

Figure 4. Horizontal distributions of Chl *a* (μg L^{-1}) and O_2 saturation (%) in the surface water of spring and summer.

3.2 Distributions of carbonate system parameters

Surface pH of the South Yellow-East China Sea region from 8.06 to 8.50, and 8.02 to 8.54 in spring and summer, with the averages of 8.20 ± 0.09 and 8.19 ± 0.09, respectively. Overall, pH increased from north to south, and the highest pH values (8.31–8.50) were mainly located in the southwestern part of the ECS. In summer, the isoline of pH was basically perpendicular to the shoreline and the low pH appeared in the coastal waters, whereas the high values of pH (8.27–8.54) were mainly observed in the river plume region (Figure 5).

Surface DIC values were in the range of 1868 to 2089 and 1826 to 2159 μmol kg^{-1}, averaging 1997 ± 54 and 1982 ± 82 μmol kg^{-1} in spring and summer, respectively. The surface DIC concentration exhibited both spatial variations and clear seasonal patterns in different subregions: a slight decreasing in the whole ECS region and an increasing trend in the SYS region from spring to summer. surface TA values were observed in the range of 2113–2318 and 2146–2410 μmol kg^{-1} in spring and summer, respectively, averaging 2244 ± 47 and 2264 ± 50 μmol kg^{-1}. In early spring, TA was homogenous in the central SYS, the middle and outer shelves of the ECS. A few higher values (2306 ± 9 μmol kg^{-1}) existed in the coastal waters of the SYS while lower values (2154 ± 29 μmol kg^{-1}) appeared in the southwestern ECS. On the other hand, TA in summer decreased from north to south in the SYS and fluctuated with a narrow range in the ECS (2247 ± 17 μmol kg^{-1}). However, the distribution of normalized TA (TA/S) decreased with the increasing salinity, which was greatly different from TA distribution (Figure 5).

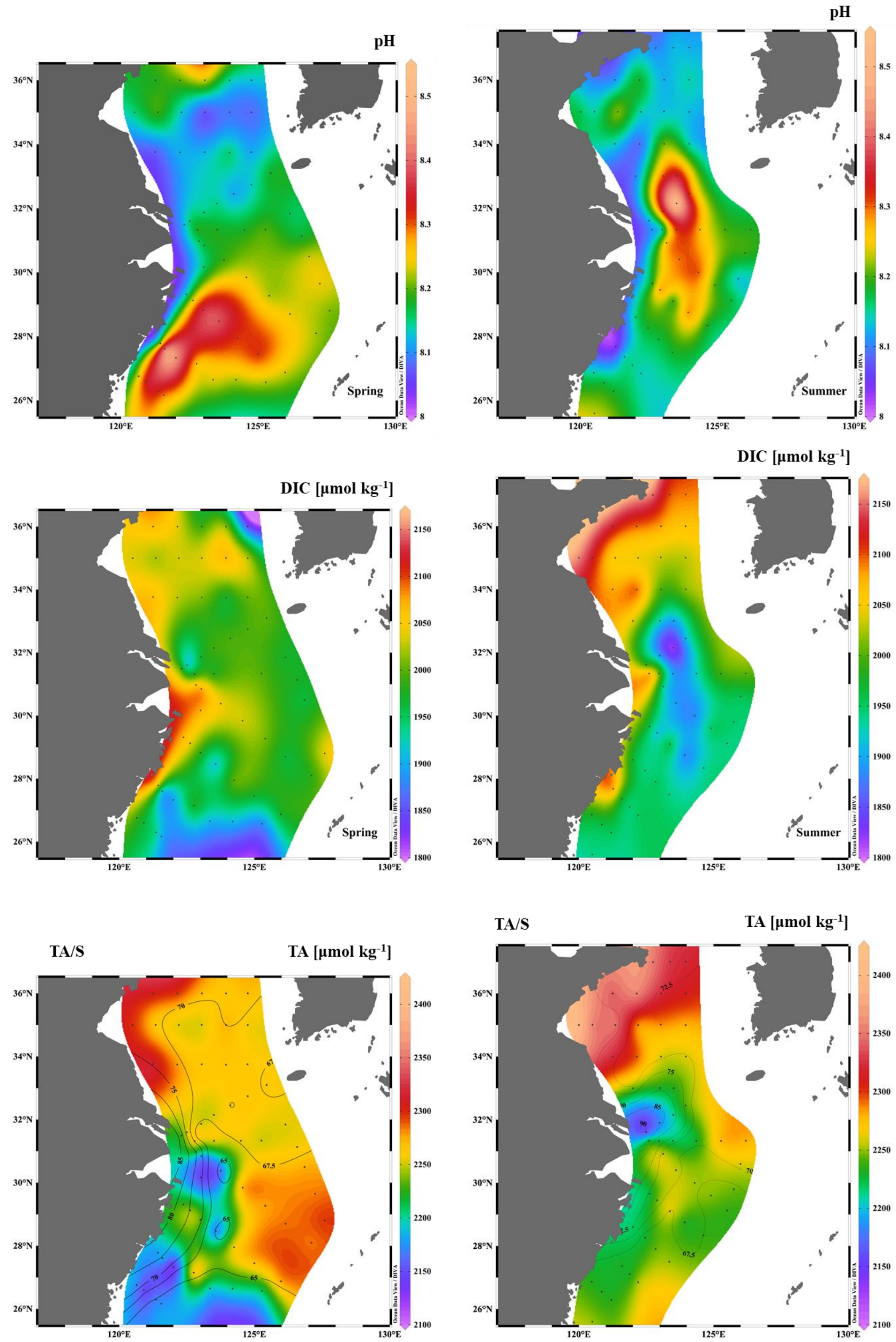

Figure 5. Horizontal distributions of pH, DIC (µmol kg^{-1}) and TA (µmol kg^{-1}) in the surface water during spring and summer. The coutour in the lower pannel represent the distribution of TA/S.

The underway pCO$_2$ data during the two cruises allow us to examine the high-resolution distribution of pCO_2 in the South Yellow-East China Sea region (Figure 6). During our sampling period, even though pCO_2 values showed similar ranges between early spring (151–689 μatm) and summer (149–709 μatm), the averaged pCO_2 values were significantly higher in summer (409 ± 71 μatm) than those in spring (360 ± 75 μatm). In spring, supersaturated pCO_2 values were observed near the Subei shoal waters (447–611 μatm), whereas pCO_2 values in the rest of SYS were generally low (258–407 μatm), except that pCO_2 in the central SYS (420–444 μatm), which was a little higher than the atmospheric pCO_2. However, in summer, pCO_2 in the SYS was generally high (>420 μatm) except that in the southern SYS, resulting from Changjiang diluted water input. In addition, few sporadic low pCO_2 values were found near the south of the Shandong Peninsula. In the river plume, pCO_2 in spring kept in a low range (<355 μatm) except in the area near the Changjiang mouth and the northwestern corner (513–689 μatm), as well as in Hangzhou Bay (421–455 μatm). To the contrary, Changjiang estuary mouth and the northwestern corner showed relatively low pCO_2 (149–386 μatm) in summer, however, high pCO_2 in the range of 420–470 μatm occurred in the coastal water near the Hangzhou Bay. The seasonal patterns in the northern and southern of ECS offshore water were different: pCO_2 in the northern ECS always showed relatively low pCO_2 in spring and summer; while southern ECS had low pCO_2 (<380 μatm) in spring and high pCO_2 in summer (>430 μatm).

Similar to the seasonality of pCO_2 in the South Yellow-East China Sea region, the air-sea CO_2 fluxes also had strong seasonal variations in the range of -18.63–19.46

and -18.03–22.61 mmol m^{-2} d^{-1}, with the average values of -4.11 ± 5.28 and 0.88 ± 5.09 mmol m^{-2} d^{-1} in spring and summer, respectively (Figure 6). The SYS and ECS were significant atmospheric CO_2 sinks in spring, with average values of -2.11 ± 4.57 and -5.56 ± 3.12 mmol m^{-2} d^{-1}, but shifted into CO_2 sources (2.35 ± 4.30 and 1.73 ± 3.05 mmol m^{-2} d^{-1}) in summer. However, the river plume always acted as a strong CO_2 sink in both spring and summer (-3.78 ± 7.44 and -5.17 ± 6.65 mmol m^{-2} d^{-1}). In addition, the Subei shoal waters was always a CO_2 source during these two surveys.

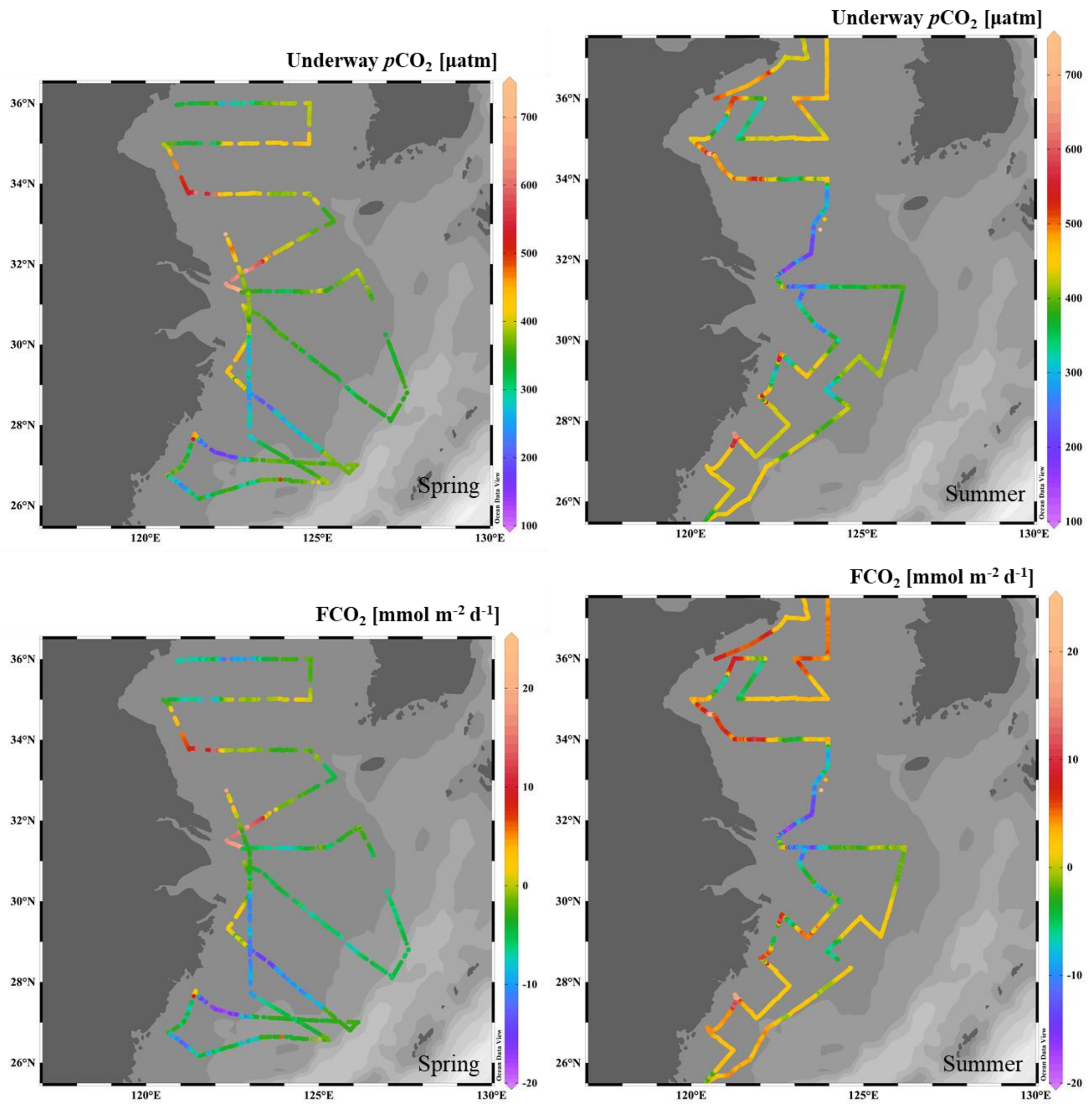

Figure 6. The trajectory of underway pCO_2 (μatm) and air-sea CO_2 flux (mmol m^{-2} d^{-1}) in the surface water during spring and summer.

4 Discussion

4.1 Classification of the water mass types

In order to understand the biogeochemistry of the South Yellow-East China Sea region and explore the influencing mechanism of carbonate system, it is necessary to describe typical water mass distributions in this study. On the basis of the temperature-salinity characteristics (Figure 7), surface waters were divided into three subregions: (1) SYS, (2) River plume and (3) ECS offshore waters. The ranges of the hydrological and carbonate system parameters in these three subregions are summarized in Table 1, and the areal distributions of these water masses are presented in Figure 2. The SYS has low temperature and moderate salinity; the ECS offshore waters are mainly impacted by the KC and TWC (Chen, 2009). The KC flows northeast along the shelf break and TWC enters the ECS through Taiwan Strait and traverses in the middle shelf (Lee & Chao, 2003). Both KC and TWC are characterized by high salinity and temperature (Chou et al., 2009). It is worth noting that the location of river plume varied from April to July under the influence of seasonal monsoons (Qi et al., 2014), which was further illustrated by the distribution of salinity (Figure 3). For example, the low salinity in the river plume was roughly confined to the nearshore from 26 to 32 °N in spring because the influence of the prevailing northeast wind (Wu et al., 2014). When it comes to summer, the

Changjiang River, carrying the nutrients, rushed out towards its northeast and formed river plume, triggering the high primary productivity there (Isobe & Matsuno, 2008).

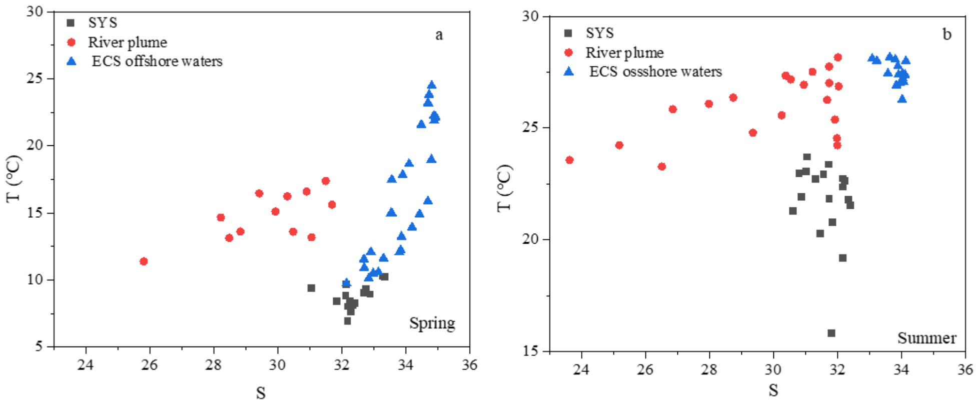

Figure 7. Temperature (T) vs. salinity (S) in surface water of the South Yellow-East China Sea region during spring (a) and summer (b) for three water masses: SYS, river plume and ECS offshore waters.

Table 1. Hydrological and carbonate parameters of the different water masses in the surface layer defined in this study.

Subregion	Longitude (°E)	Latitude (°N)	T (°C)	S	Chl *a* (μg L^{-1})	DO Saturation (%)
Spring SYS	120.0–125.5	33.0–36.0	6.91–10.25	31.05–33.36	0.07–1.93	101–125
			(8.71 ± 0.91)	(32.39 ± 0.55)	(0.59 ± 0.51)	(106 ± 6)
River plume	122.0–123.5	28.0–32.0	11.37–17.38	25.81–32.26	0.23–8.80	100–167
	120.0–122.0	26.0–28.0	(14.55 ± 1.85)	(29.92 ± 1.76)	(2.66 ± 2.97)	(117 ± 22)

ECS offshore	123.5–127.6	28.0–33.0	9.75–24.47	32.15–34.94	0.03–1.88	98–141
	122.0–126.2	25.5-28.8	(16.47 ± 5.01)	(33.90 ± 0.82)	(0.49 ± 0.41)	(106 ± 9)
Summer						
SYS	120.0–125.5	33.0–37.5	15.82–23.70	30.61–32.40	0.16–3.03	82–188
			(21.71 ± 1.87)	(31.64 ± 0.57)	(1.00 ± 0. 98)	(156 ± 21)
River plume	122.0–124.3	29.0–33.0	23.28–27.76	23.63–31.74	0.57–8.22	122–173
			(25.98 ± 1.43)	(29.12 ± 2.56)	(2.74 ± 2.41	(150 ± 18)
ECS offshore	124.3–126.2	29.0–33.0	24.23–28.17	31.93–34.14	0.13–1.21	120–174
	120.0–125.5	25.5–29.0	(27.08 ± 1.15)	(33.37 ± 0.86)	(0.52 ± 0.36)	(149 ± 10)

(Table 1 continued)

Subregion	pH	DIC (μmol kg^{-1})	TA (μmol kg^{-1})	Underway pCO_2 (μatm)	FCO_2 (mmol m^{-2} d^{-1})
Spring					
SYS	8.06–8.24	1965–2071	2251–2318	258–611	-12.44–14.08
	(8.14 ± 0.05)	(2028 ± 30)	(2275 ± 20)	(393 ± 61)	(-2.11 ± 4.57)
River plume	8.11–8.50	1868–2089	2113–2259	170–689	-17.48–19.46
	(8.24 ± 0.13)	(2001 ± 78)	(2195 ± 47)	(365 ± 104)	(-3.78 ± 7.44)
ECS offshore	8.11–8.39	1877–2046	2160–2297	151–411	-18.62–-0.68
	(8.22 ± 0.06)	(1976 ± 41)	(2250 ± 39)	(336 ± 44)	(-5.56 ± 3.12)
Summer					
SYS	8.08–8.36	1997–2159	2245–2410	261–709	-9.79–22.61
	(8.16 ± 0.07)	(2078 ± 47)	(2316 ±43)	(432 ± 60)	(2.35 ± 4.30)
River plume	8.10–8.54	1826–1967	2146–2259	149–564	-18.03–11.99
	(8.26 ± 0.12)	(1905 ± 34)	(2224 ± 28)	(326 ± 92)	(-5.17 ± 6.65)
ECS offshore	8.02–8.31	1879–2004	2223–2280	296–664	-7.11–19.02
	(8.18 ± 0.06)	(1954 ± 26)	(2247 ± 17)	(420 ± 44)	(1.73 ±3.05)

4.2 The carbonate parameters variability in subregions

Two opposite trends can be obtained from the TA-S and DIC-S scatter plots (Figure 8): one with a negative relationship encompassing the data from the SYS and the other with a positive relationship including the river plume samples. Both regressions converge towards the ECS offshore waters and represent the mixing of these three water masses. The corresponding water mass with high TA and DIC originated from the SYS which could be attributed to the very high TA and DIC discharges of the Yellow River, which has intensive carbonate weathering and erosion in the drainage basin (Liu et al., 2014; Zhang et al., 1990). The positive relationship was characterized by the mixing between the Changjiang River and ECS offshore waters. However, DIC near the Hangzhou Bay was little high in spring ((>2000 μmol kg^{-1}, shaded grey in Figure 8a), because the DIC-enrich TWC bottom water flowed northward and extended to around 30°N (Li et al., 2012), then mixed well with the surface water in the water column, leading to the high DIC in spring.

DIC and TA concentrations in spring were low near the Zhe-Min Coastal Current (Yellow shaded circles in Figures 8a and 8c). It could be related to the river inputs with low DIC and TA values, such as Minjiang River with low DIC concentration of about 500 μmol L^{-1} in April (Qian et al., 2019). Moreover, the high TA/S values (Figure 5) with the low salinity (Figure 3) in the coastal waters also indicated the influences of terrestrial inputs on DIC and TA values (Jiang et al., 2014). On the other hand, the nutrient enrichment phenomenon was observed in the Zhe-Min Coastal Current, which was caused by river runoff and coastal upwelling, enhancing the primary production and lowering DIC values in this area (Wang & Wang, 2007).

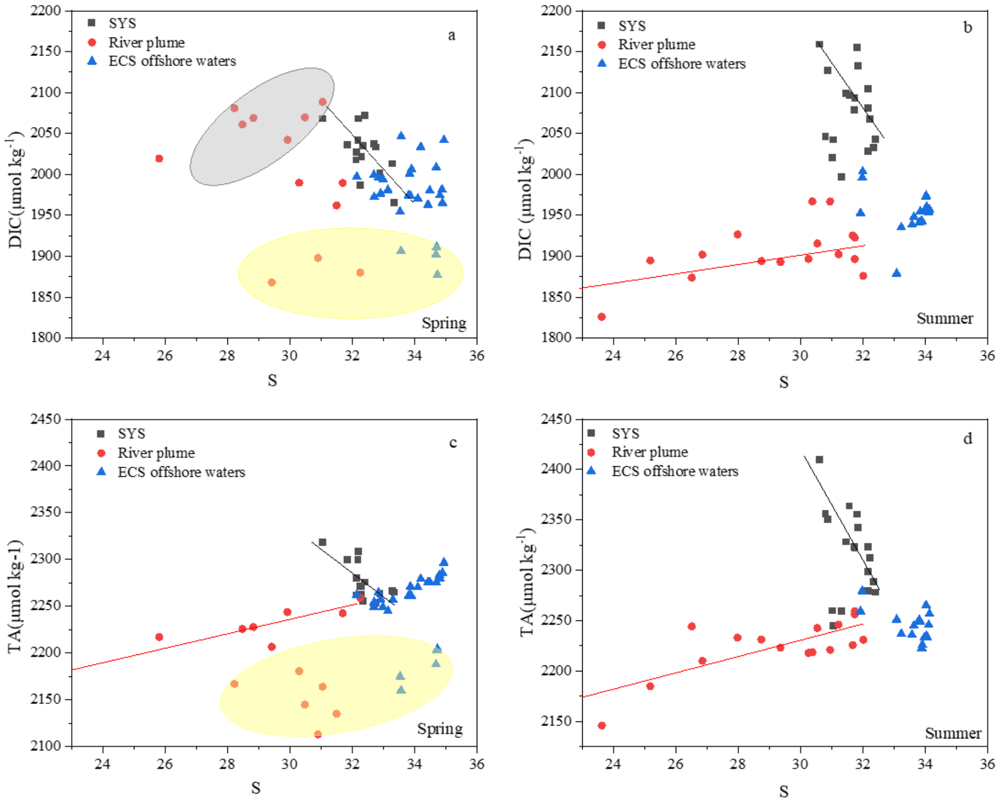

Figure 8. The relationships between surface DIC vs salinity (upper panel) and TA vs salinity (lower panel) in spring and summer in three water masses. The grey shaded circle represents the stations near the Hangzhou Bay and the yellow shaded circles represent the stations in the Zhe-Min Coastal Current.

4.3 Temperature and non-temperature effects on pCO$_2$ variability

Field investigations conducted in the global oceans indicate that temperature is one of the most important factors controlling seawater CO_2 (Millero, 1995; Takahashi et al., 2002) as a consequence of the dependence of the solubility of CO_2 with the temperature (Weiss, 1974). Meanwhile, field observations in the productive continental shelf seas have demonstrated that biological activity also plays a key role in carbonate characteristics of ocean systems (Takahashi et al., 2002; Thomas et al., 2005; Zhai et al., 2014). In order to quantify the relative importance of temperature and biological effects on the seasonal changes of pCO_2 from spring to summer, we calculated the temperature effect in all three subregions with the method proposed by Takahashi et al. (2002). Briefly, the temperature effect can be removed by normalizing pCO_2 data at each station to an average temperature (19.31℃) for spring and summer seasons:

$$pCO_2 \text{ at } T_{mean} = pCO_{2,\,obs} * \exp\,[0.0423\,(T_{mean} - T_{obs})], \qquad (5)$$

where T is the temperature in °C, and the subscripts “mean” and “obs” indicate the average and observed values, respectively. Thus, the biological activity effect on pCO_2 in different subregions described above are discussed based on the relationship between normalized pCO_2 (npCO_2, normalized to average temperature in this study based on the equation (5)) and Chl *a* in each station.

In the SYS, the different trends between underway pCO_2 and SST in spring and summer were found (Figure 9a): a positive correlation (r = 0.32, p < 0.001) in the middle and north parts (north of the transect C) in April, and negative correlations in the southern part (south of the transect C) in April (r = -0.72, p < 0.001) and in summer (r = -0.46, p < 0.001). The positive correlation in the north and middle parts in spring indicated that temperature was the leading role in the pCO_2 distribution, which was also found by Liu et al. (2008) in late March and May. Underway pCO_2 decreased from the west to east along the transect C (Figure 6), which was consistent with the results of high pCO_2 in the southwestern SYS (Qu et al., 2017) and low pCO_2

in the southeastern part (Choi et al., 2019). It is due to the fact that the southwest SYS was occupied by the Subei shoal waters with extremely high concentration of suspended sediment (Wang et al., 2011a) while high biological activity in the southeast SYS (Choi et al., 2019). The negative correlation in July suggested that temperature was no longer the primary factor in controlling the pCO_2 variability, it tended to be ascribed to the biological activity in this study area (Qu et al., 2014; Zhang et al., 2010). The low pCO_2 in the southern part was mainly affected by the Changjiang diluted water, which could be seen from the positive correlation between pCO_2 and salinity in summer (Figure 9b). Similar negative relationships of pCO_2 and temperature were also reported in the SYS in summer by Qu et al. (2014) and Zhang et al. (2010) and the inner and middle shelves of the ECS in winter (Chou et al., 2011). Therefore, the controlling mechanisms on pCO_2 variation in the SYS varied with different seasons.

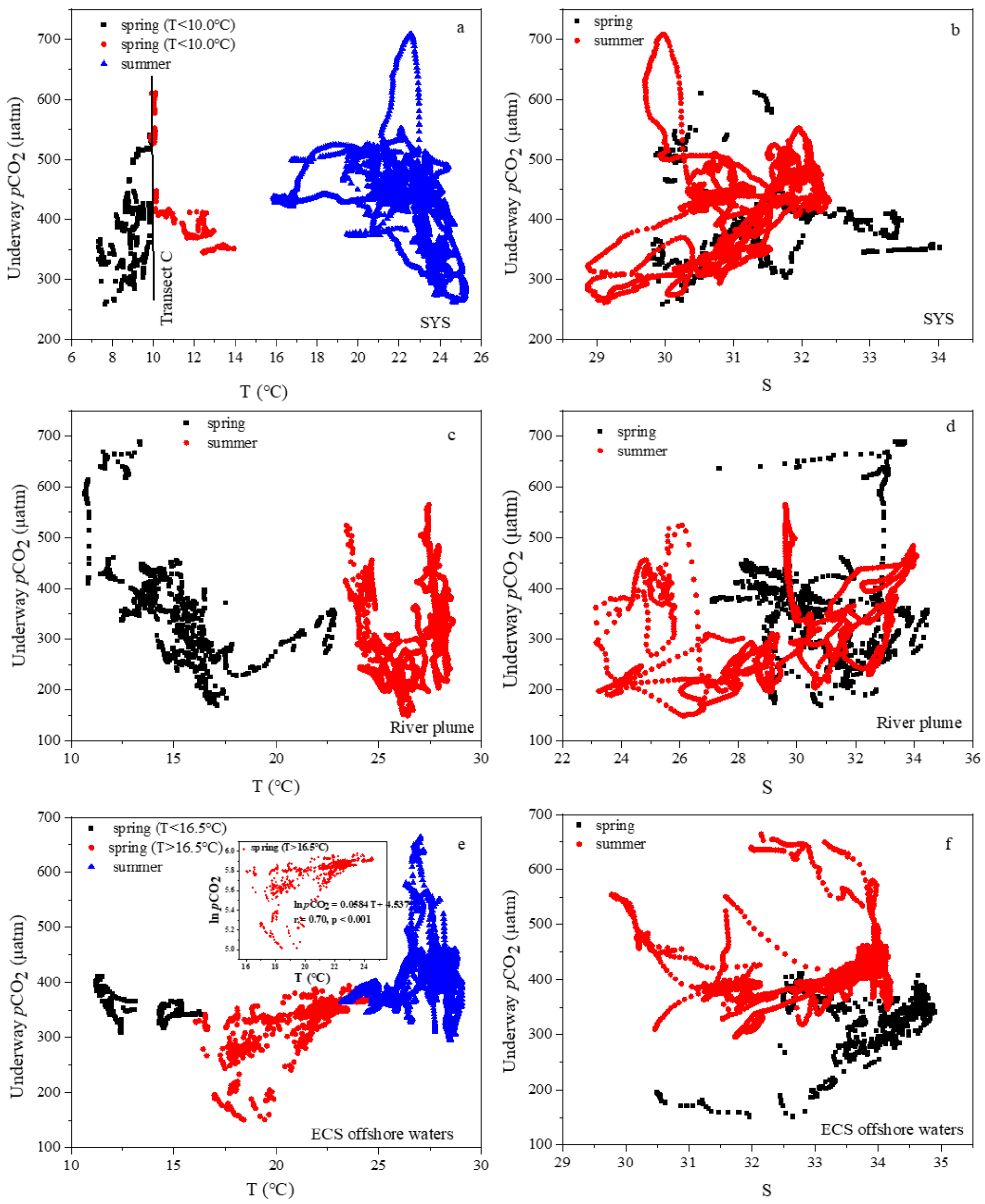

Figure 9. Relationships among underway pCO_2, temperature and salinity in three subregions in spring and summer. The insert graph in panel (e) shows the relationship between ln pCO_2 and temperature when temperature is higher than 16.5°C in the ECS offshore waters ($\partial\ pCO_2 / \partial\ T = 0.0584$ °C^{-1}).

The negative relationship between $npCO_2$ and Chl *a* in spring ($r = -0.59$, n = 14, $p < 0.05$) and no conspicuous relationship between them in the SYS during summer

(Figure 10a) demonstrated that the effect of biological production on CO_2 sequestration processes varied with seasons, which was also found by the observation of Qu et al. (2017) in spring and summer of the SYS, 2011. Noted that a weak CO_2 source replaced a significant CO_2 sink in the central SYS in spring (Figure 6), which was opposed to the results of Qu et al. (2014). The reason could be attributed to the fact that a strong vertical mixing still existed in the late-March, and a little bit high pCO_2 in the central SYS thus was caused by the upwelling of CO_2-riched Yellow Sea Warm Current, which was characterized by high-temperature saline water (Figure S1, see the supplement). Moreover, the onset of the spring phytoplankton bloom in the central SYS usually started from April (Jin et al., 2013; Liu et al., 2015). Therefore, low biological uptake in the central SYS was not strong enough to offset the enhanced pCO_2 from the upwelling of the CO_2-enriched bottom water. The net result was elevated pCO_2 value in the central SYS in early spring.

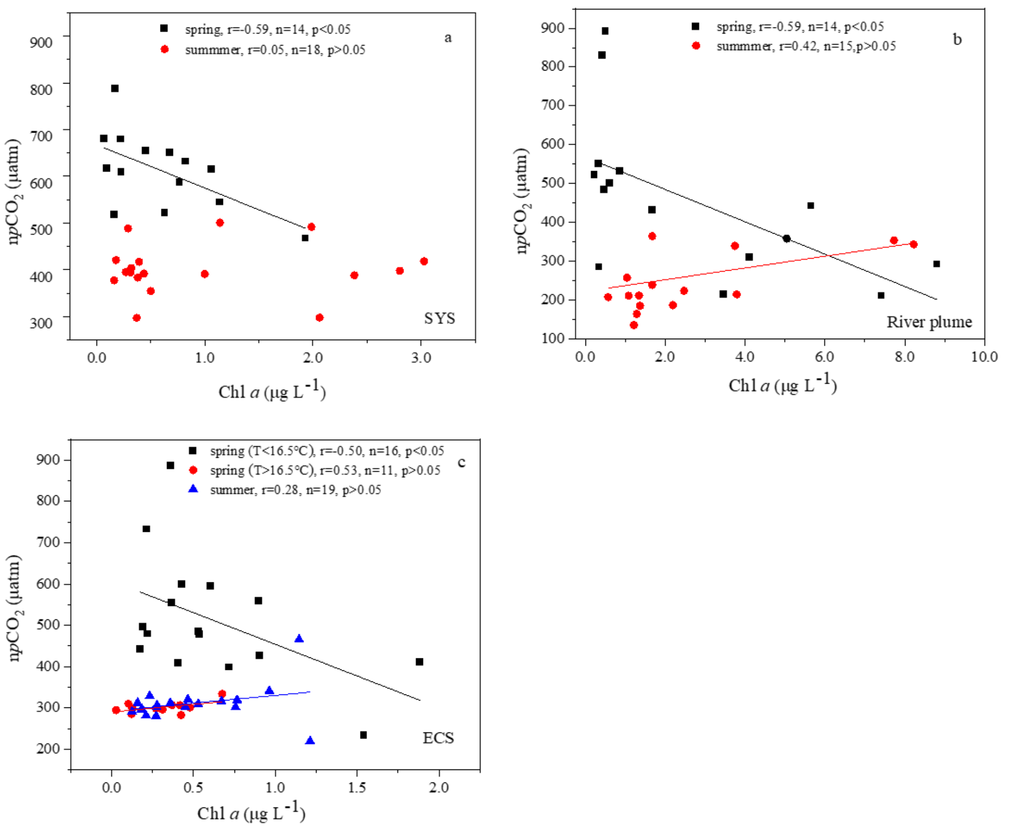

Figure 10. Relationship n$p$$CO_2$ and Chl *a* in spring and summer in three water masses: SYS (a), River plume (b) and ECS offshore waters (c).

In the plume area, the relationship of underway pCO_2 and SST in spring is negative but random in summer, while the relationship of pCO_2 and salinity in spring is random but positive in summer (Figures 9c and 9d). In summer, the positive relationship between pCO_2 and salinity was similar to the result of the cruise in July 2007, which was found by Zhai and Dai (2009). Relatively high pCO_2 (Figure 9d) near the Changjiang River mouth (S= 24–26) was mainly subjected to the physical mixing effect. Moreover, photosynthesis was at a low level given the light limitation and strong vertical mixing in the turbid area in spite of high concentration nutrients supply, therefore resulting in high pCO_2 distribution (He et al., 2013; Zhai et al., 2007). Besides, this area was also more affected by the SYS through the Yellow Sea Coastal Current in spring that carried higher CO_2 water southward, thereby resulting in high pCO_2 in the northwest corner of the Changjiang estuary with moderate salinity (Su, 1998). In the outer estuary, low pCO_2 values were distributed in the northeast of the Changjiang estuary. It demonstrated in addition to the physical processes but reinforcement of biological action also greatly affected pCO_2 dynamics. In the south branch of the Changjiang estuary, on one hand, high primary production in this region was fueled by abundant nutrients with the Changjiang River supply, thus leading to biological CO_2 uptake and low pCO_2; On the other hand, the upwelling carrying CO_2-rich water, which from the flow-northward TWC bottom water, mixed with the surface water and thereby elevated pCO_2 (Wang et al., 2011b). Therefore, the upwelling effect canceled out the intensive biological activity to some extent, then resulting in pCO_2 of the south branch slightly higher than the northwest branch (Figure 6).

In spring, the overall random relationship between pCO_2 and salinity as well as the relatively narrow salinity range revealed a strong mixing in water column. Moreover, the negative correlation between pCO_2 and SST in spring also suggested that the water mixing between high-pCO_2/low-temperature river water and low-pCO_2/high-temperature ECS water. As for Zhe-Min Coastal Current, intensive primary production occurred with the high nutrients loading from the Changjiang River leading to low pCO_2 values (He et al., 2013; Guo et al., 2015). The negative relationship between n$p$$CO_2$ and Chl *a* in spring (r = -0.59, n = 14, $p < 0.05$, Figure 10b) demonstrated that biological activity was also the main driver on the $p$$CO_2$ distribution.

All summer stations in the ECS were confined to the shelf break of the ECS, while some spring stations were expanded to the outer shelf of the ECS, which was influenced by the KC and open ocean to some extent. The southern and outer shelf of ECS was characterized by warm and saline water with the influences of TWC and KC. In spring, considering that the isotherm of 16.5 °C coincided with the depth contour of 100m in the ECS, the relationship underway $p$$CO_2$ and SST in the ECS offshore waters was divided into two parts to discuss (Figure 9e): one is the negative correlation in the inner and middle shelves with SST < 16.5 °C (r = -0.49, $p < 0.001$); another is the significant positive correlation in the outer shelf with SST > 16.5 °C (r = 0.74, $p < 0.001$). This indicated that the $p$$CO_2$ variation in the outer shelf of the ECS was mainly dominated by temperature and the apparent coefficient of temperature effect on surface seawater $p$$CO_2$ was 0.0584 $°C^{-1}$, which was higher than that of the 0.0423 $°C^{-1}$ determined for North Atlantic surface water by Takahashi et al. (1993). This suggested that the temperature effect on seawater $p$$CO_2$ was enhanced by other important processes (i.e. mixing with Kuroshio subsurface CO_2-rich water). Moreover, the apparent temperature coefficient was similar to that in South Atlantic Bight (0.058 $°C^{-1}$; Jiang et al., 2008), and higher than that in northern South China Sea (0.024, 0.049 and 0.03 $°C^{-1}$ in spring, autumn and winter, respectively; Tseng et al., 2007), and northern Yellow Sea (0.0205 $°C^{-1}$; Xu et al., 2016). In the inner and middle shelves of the ECS, the combined influence of the physical mixing and the biological activity masked the effects of temperature on the pCO_2 distribution. The negative relationship between npCO_2 and Chl *a* (r = -0.50, n = 16, $p < 0.05$) also showed that the phytoplankton production mainly led to the pCO_2 variation in the inner and middle shelves. Moreover, the positive correlation of the pCO_2 and salinity in spring (Figure 9f) could be an evidence to affirm the intrusion of high salinity CO_2-rich KC water to the ECS.

4.4 Air-sea CO_2 fluxes in subregions and implication

With the three subregions categorized in the South Yellow-East China Sea region, the seasonality variation of both pCO_2 and air-sea CO_2 fluxes were found in each individual region. Theoretically, the variation of the CO_2 flux was mainly attributed to the variability in ΔpCO_2 and wind speed (Jiang et al., 2008). In the present study, we used the same reanalyzed monthly averaged wind speed from ECMWF to calculate the CO_2 flux inside each cruise. Therefore, there was no spatial pattern in the intra-seasonal variation of the wind speed and the flux difference was solely ascribed to the ΔpCO_2. Therefore, all above factors that influencing pCO_2 variability also affected the distributions of CO_2 flux.

In this study, the SYS served as a CO_2 sink in early spring and a CO_2 source in summer with the average air-sea CO_2 flux of -2.11 ± 4.57 and 2.35 ± 4.30 mmol m^{-2} d^{-1}, respectively. This was in good agreement with the findings in the surveys of Xue et al. (2011) and Qu et al. (2017). To be more specific, it was unquestionable that the

SYS served as a CO_2 sink in spring because of low temperature and spring bloom. The trajectory of underway pCO_2 data clearly verified that spring pCO_2 in the SYS was all undersaturated except for the Subei shoal in the southwest SYS (Figure 6). However, in summer, a strong CO_2 sink in the SYS from the June gradually reduced to a weak sink or source in July and further converted to an obvious CO_2 source in August, according to the compilation of our data and the results from Qu et al. (2014, 2017). In the SYS, the outbreak of *Ulva prolifera* bloom between the April and June every year absorbs a large amount of CO_2, which promotes the SYS to become a temporary CO_2 sink in early summer (Van Alstyne et al., 2015), then the degradation of the *U. prolifera* in the mid-July to late August also accelerate it to act as a CO_2 source (Deng et al., 2018). Therefore, the temporal changes of pCO_2 and CO_2 flux are combined results from biological activity, the Changjiang River plume and the upwelling of the Yellow Sea Cold Water. An exception is that the southeastern SYS along the Korean coast was a net strong CO_2 sink during spring, summer and fall, whereas it was a net weak source during winter (Choi et al., 2019). The sharp contrast in CO_2 fluxes could be attributed to regional variations in magnitude and the terrestrial influences, especially the influences of Changjiang and Yellow Rivers on the western SYS in summer. In short, the factors affecting the pCO_2 distribution and CO_2 flux, especially in summer, are complicated, and more detailed mechanisms for these changes in summer need further intense investigation.

As a whole, the river plume region always acted as a CO_2 sink with the fluxes of -3.78 ± 7.44 and -5.17 ± 6.65 mmol m^{-2} d^{-1} from spring to summer. The estimated

CO_2 flux in summer were close to those of Zhai and Dai (2009) (-8.8 ± 5.8 and -4.9 ± 4.0 mmol m^{-2} d^{-1} in spring and summer) and multiple observations by Guo et al. (2015) (-10.7 ± 8.2 and -6.5 ± 10.7 mmol m^{-2} d^{-1} in spring and summer), whereas the CO_2 flux we calculated in spring was lower than those. It could be ascribed to the fact that spring is the transitional season from winter to summer and the plume area is also the transitional zone from the inland to the ECS. Thus, the magnitude of CO_2 flux changes associated with many factors, including wind speed, biological activity and river discharge, etc. Therefore, the estimated CO_2 fluxes in this study are reasonable in comparison with the CO_2 fluxes in spring from multiple observations, such as those of Zhai and Dai (2009) and Guo et al. (2015). As for the ECS, the northern ECS always was a sink in both spring and summer, due to the jointly impacts of primary production and Changjiang River input (Kim et al., 2013), while the southern ECS shifted the CO_2 sink in spring to source in summer with the increasing intrusion of KC and TWC in summer. Overall, the ECS offshore water was also a strong sink in spring with an average CO_2 flux of -5.56 ± 3.12 mmol m^{-2} d^{-1}. When it comes to summer, it turned into a CO_2 source with the seasonal average CO_2 flux of 1.73 ± 3.05 mmol m^{-2} d^{-1}, which might be due to the fact that high temperature in the ECS offshore waters, especially in the southern ECS, contributed to the high pCO_2 and a CO_2 source in summer. This is also in good consistency with the flux reported by Guo et al. (2015) in summer.

5 Conclusion

Based on the hydrological and carbonate parameters observations with high spatial resolution in the South Yellow-East China Sea region from spring and summer cruises, the results showed that DIC and TA values decreased generally from nearshore to offshore, moreover, the low TA and DIC values as well as high pH, occurred in the river plume, especially in the Zhe-Min Coastal Current in spring. The DIC and TA values in the SYS were higher than those in the ECS due to the Yellow River with intensive carbonate weathering and erosion in the drainage basin. The South Yellow Sea and East China Sea, as a whole, turned from an important CO_2 sink in spring to a weak CO_2 source in summer, Specifically, the air-sea CO_2 flux displayed large spatial and temporal variations in three subregions: CO_2 sinks in the SYS and ECS offshore water converted into sources from spring to summer, while the river plume always served as a CO_2 sink both in spring and summer. The controlling factors of pCO$_2$ differ in different regions and seasons. In general, temperature and biological activity were the primary drivers in controlling the pCO$_2$ variability in the SYS, and primary production was more important than temperature in summer. For the river plume area, pCO$_2$ distribution was largely controlled by physical mixing and biological activity, which could be attributed to the Changjiang runoff with high nutrients supply, while temperature was the dominant factor in the outer shelf of the ECS as the high-temperature KC saline water always occupied in the region.

This study improved the understand of sea surface carbonate chemistry dynamics in the two adjacent margin seas with different physical conditions and may also help to better understand the chemical dynamics in many other marine systems. To better understand the role of the continental shelf seas in the global carbon cycle, more comprehensive surveys and researches of direct pCO_2 measurements in the entire South Yellow Sea and East China Sea, especially the seasons (autumn and winter) with weak primary production, are needed.

Acknowledgements

This work was financially supported by the National Key Research and Development Program of China (no. 2016YFA0601301) and the National Natural Science Foundation of China (no. 41676065). All authors have no conflict of interest. The dataset used in this study has been submitted to the Mendeley Data. However, data archiving is underway and thus we upload a copy of data as Supporting Information for review purpose. The authors thank the captain and crews of the R/V "*Dongfanghong II*" for their help during the in-situ investigation. We are also thankful to Hongjie Wang and Liang Xue for suggestions for this manuscript.

References

Bauer, J. E., Cai, W. J., Raymond, P. A., Bianchi, T. S., Hopkinson, C. S., & Regnier, P. A. (2013). The changing carbon cycle of the coastal ocean. *Nature*, 504(7478), 61–70. https://doi.org/10.1038/nature12857

Borges, A. V., Delille, B., & Frankignoulle, M. (2005). Budgeting sinks and sources of CO_2 in the coastal ocean: Diversity of ecosystems counts. *Geophysical research letters*, 32(14), L14601. https://doi.org/10.1029/2005GL023053

Bozec, Y., Thomas, H., Elkalay, K., & de Baar, H. J. (2005). The continental shelf pump for CO_2 in the North Sea-evidence from summer observation. Marine Chemistry, 93(2-4), 131–147. https://doi.org/10.1016/j.marchem.2004.07.006

Cai, W. J. (2011). Estuarine and coastal ocean carbon paradox: CO_2 sinks or sites of terrestrial carbon incineration? *Annual Review of Marine Science*, 3, 123–145. https://doi.org/10.1146/annurev-marine-120709-142723

Cai, W. J., Dai, M. H., & Wang, Y. C. (2006). Air-sea exchange of carbon dioxide in ocean margins: A province-based synthesis. *Geophysical Research Letters*, 33(12), L12603. https://doi.org/10.1029/2006GL026219

Cai, W. J., Dai, M. H., Wang, Y. C., Zhai, W. D., Huang, T., Chen, S. T., et al. (2004). The biogeochemistry of inorganic carbon and nutrients in the Pearl River estuary and the adjacent Northern South China Sea. *Continental Shelf Research*, 24(12), 1301–1319. https://doi.org/10.1016/j.csr.2004.04.005

Cai, W. J., Hu, X. P., Huang, W. J., Jiang, L. Q., Wang, Y. C., Peng, T. H., & Zhang, X. (2010). Alkalinity distribution in the western North Atlantic Ocean margins. *Journal of Geophysical Research: Oceans*, 115(C8), C08014. https://doi.org/10.1029/2009JC005482

Cai, W. J., Wang, Z. A., & Wang, Y. C. (2003). The role of marsh-dominated heterotrophic continental margins in transport of CO_2 between the atmosphere, the land-sea interface and the ocean. *Geophysical Research Letters*, 30(16), 1849. https://doi.org/10.1029/2003GL017633

Chen, C. T. A. (2003). New vs. export production on the continental shelf. *Deep Sea Research Part II: Topical Studies in Oceanography*, 50(6–7), 1327–1333.

https://doi.org/10.1016/S0967-0645(03)00026-2

Chen, C. T. A. (2009). Chemical and physical fronts in the Bohai, Yellow and East China seas. *Journal of Marine Systems*, 78(3), 394–410. https://doi.org/10.1016/j.jmarsys.2008.11.016

Choi, Y., Kim, D., Cho, S., & Kim, T. W. (2019). Southeastern Yellow Sea as a sink for atmospheric carbon dioxide. *Marine pollution bulletin*, 149, 110550. https://doi.org/10.1016/j.marpolbul.2019.110550

Chou, W. C., Gong, G. C., Sheu, D. D., Hung, C. C., & Tseng, T. F. (2009). Surface distributions of carbon chemistry parameters in the East China Sea in summer 2007. *Journal of Geophysical Research: Oceans*, 114, C07026. https://doi.org/10.1029/2008JC005128

Chou, W. C., Gong, G. C., Tseng, C. M., Sheu, D. D., Hung, C. C., Chang, L. P., & Wang, L. W. (2011). The carbonate system in the East China Sea in winter. *Marine Chemistry*, 123(1–4), 44–55. https://doi.org/10.1016/j.marchem.2010.09.004

Dai, M. H., Cao, Z. M., Guo, X. H., Zhai, W. D., Liu, Z. Y., Yin, Z. Q., et al. (2013). Why are some marginal seas sources of atmospheric CO_2?. *Geophysical Research Letters*, 40(10), 2154–2158. https://doi.org/10.1002/grl.50390

DeGrandpre, M. D., Olbu, G. J., Beatty, C. M., & Hammar, T. R. (2002). Air-sea CO_2 fluxes on the US Middle Atlantic Bight. *Deep sea research part II: Topical studies in oceanography*, 49(20), 4355–4367. https://doi.org/10.1016/S0967-0645(02)00122-4

Deng, X., Liu, T., Liu, C. Y., Liang, S. K., Hu, Y. B., Jin, Y. M., & Wang, X. C. (2018). Effects of *Ulva prolifera* blooms on the carbonate system in the coastal waters of Qingdao. *Marine Ecology Progress Series*, 605, 73–86. https://doi.org/10.3354/meps12739

Dickson, A. G. (1994). Determination of dissolved oxygen in sea water by Winkler titration. *WHP Operations and Methods*, 1–14.

Goyet, C., Millero, F. J., O'Sullivan, D. W., Eischeid, G., McCue, S. J., & Bellerby, R. G. J. (1998). Temporal variations of pCO_2 in surface seawater of the Arabian Sea in 1995. *Deep Sea Research Part I: Oceanographic Research Papers*, 45(4–5), 609–623. https://doi.org/10.1016/S0967-0637(97)00085-X

Guo, X. H., Zhai, W. D., Dai, M. H., Zhang, C., Bai, Y., Xu, Y., et al. (2015). Air-sea CO_2 fluxes in the East China Sea based on multiple-year underway observations. *Biogeosciences*, 12(18), 5495–5514. https://doi.org/10.5194/bg-12-5495-2015

He, X., Bai, Y., Pan, D., Chen, C. T., Cheng, Q., Wang, D., & Gong, F. (2013). Satellite views of the seasonal and interannual variability of phytoplankton blooms in the eastern China seas over the past 14 yr (1998–2011). *Biogeosciences*, 10(7), 4721–4739. https://doi.org/10.5194/bg-10-4721-2013

Huang, W. J., Wang, Y., & Cai, W. J. (2012). Assessment of sample storage techniques for total alkalinity and dissolved inorganic carbon in seawater. *Limnology and oceanography: Methods*, 10(9), 711–717. https://doi.org/10.4319/lom.2012.10.711

Isobe, A., & Matsuno, T. (2008). Long-distance nutrient-transport process in the Changjiang river plume on the East China Sea shelf in summer. *Journal of Geophysical Research: Oceans,* 113, C04006. https://doi.org/10.1029/2007JC004248

Jiang, L. Q., Cai, W. J., Wanninkhof, R., Wang, Y., & Lüger, H. (2008). Air-sea CO_2 fluxes on the US South Atlantic Bight: Spatial and seasonal variability. *Journal of Geophysical Research: Oceans*, 113, C07019. https://doi.org/10.1029/2007JC004366

Jiang, Z. P., Tyrrell, T., Hydes, D. J., Dai, M., & Hartman, S. E. (2014). Variability of alkalinity and the alkalinity-salinity relationship in the tropical and subtropical surface ocean. *Global Biogeochemical Cycles*, 28(7), 729 – 742. https://doi.org/10.1002/2013GB004678

Jin, J., Liu, S. M., Ren, J. L., Liu, C. G., Zhang, J., & Zhang, G. L. (2013). Nutrient dynamics and coupling with phytoplankton species composition during the spring blooms in the Yellow Sea. *Deep Sea Research Part II: Topical Studies in Oceanography*, 97, 16–32. https://doi.org/10.1016/j.dsr2.2013.05.002

Kempe, S., & Pegler, K. (1991). Sinks and sources of CO_2 in coastal seas: the North Sea. *Tellus B*, 43(2), 224–235. https://doi.org/10.1034/j.1600-0889.1991.00015.x

Kim, D., Choi, S. H., Shim, J., Kim, K. H., & Kim, C. H. (2013). Revisiting the Seasonal Variations of Sea-Air CO_2 Fluxes in the Northern East China Sea. *Terrestrial, Atmospheric & Oceanic Sciences,* 24(3), 409-419.

https://doi.org/10.3319/TAO.2012.12.06.01(Oc)

Lee, H. J., & Chao, S. Y. (2003). A climatological description of circulation in and around the East China Sea. *Deep Sea Research Part II: Topical Studies in Oceanography*, 50(6–7), 1065–1084. https://doi.org/10.1016/S0967-0645(03)00010-9

Li, W., Wang, Y. H., Wang, J. N., & Wei, H. (2012). Distributions of water masses and hydrographic structures in the Yellow Sea and East China Sea in spring and summer 2011. *Oceanologia et Limnologia Sinica*, 3, 615–623. (In Chinese with English abstract)

Li, Y., Yang, X., Han, P., Xue, L., & Zhang, L. (2017). Controlling mechanisms of surface partial pressure of CO_2 in Jiaozhou Bay during summer and the influence of heavy rain. *Journal of Marine Systems*, 173, 49–59. https://doi.org/10.1016/j.jmarsys.2017.04.006

Liu, C., Zhang, C., Yang, X., Gong, H., & Zhang, Z. (2008). A multilayer study of $p$$CO_2$ in the surface waters of the Yellow and South China Seas in spring and the sea-air carbon dioxide flux. *Journal of Ocean University of China*, 7(3), 263–268. https://doi.org/10.1007/s11802-007-0263-2

Liu, X., Huang, B., Huang, Q., Wang, L., Ni, X., Tang, Q., et al. (2015). Seasonal phytoplankton response to physical processes in the southern Yellow Sea. *Journal of Sea Research*, 95, 45–55. https://doi.org/10.1016/j.seares.2014.10.017

Liu, Z., Zhang, L., Cai, W. J., Wang, L., Xue, M., & Zhang, X. (2014). Removal of dissolved inorganic carbon in the Yellow River Estuary. *Limnology and oceanography*, 59(2), 413–426. https://doi.org/10.4319/lo.2014.59.2.0413

Mackenzie, F. T., Bewers, J. M., Charlson, R. J., Hofmann, E. E., Knauer, G. A., Kraft, J. C., et al. (1991). What is the importance of ocean margin processes in global change?. *in Ocean Margin Processes in Global Change*, editedby R. F. C. Mantoura, J. M. Martin, and R. Wollast, pp. 433–454, JohnWiley, New York, 1991. https://doi.org/10013/epic.12626

Millero, F. J. (1995). Thermodynamics of the carbon dioxide system in the oceans. *Geochimica et Cosmochimica Acta*, 59(4), 661–677. https://doi.org/10.1016/0016-7037(94)00354-O

Omar, A. M., Olsen, A., Johannessen, T., Hoppema, M., Thomas, H., & Borges, A. V. (2010). Spatiotemporal variations of $f$$CO_2$ in the North Sea. *Ocean Science*. 6(1), 77–89. http://dx.doi.org/10.5194/os-6-77-2010

Parsons, T. R., Maita, Y., & Lalli, C. M. (1984). Amanual of chemical and biological methods for seawater analysis. *Oxford: Pergamon*, 1, 173.

Pierrot, D., Neill, C., Sullivan, K., Castle, R., Wanninkhof, R., Lüger, H., et al. (2009). Recommendations for autonomous underway $p$$CO_2$ measuring systems and data-reduction routines. *Deep Sea Research Part II: Topical Studies in Oceanography*, 56(8–10), 512–522. https://doi.org/10.1016/j.dsr2.2008.12.005

Qi, J., Yin, B., Zhang, Q., Yang, D., & Xu, Z. (2014). Analysis of seasonal variation of water masses in East China Sea. *Chinese Journal of Oceanology and Limnology*, 32(4), 958–971. https://doi.org/10.1007/s00343-014-3269-1

Qian, W., Chen, Y., Yang, L. M., Peng., Y. Z., Zhang, L., Li, T. Y., & Jiang, M. H. (2019). Carbon Fraction and Fluxes in the Lower Reach of Minjiang River. Research of Environmental Sciences, 32(4), 648–653. (In Chinese with English abstract)

Qu, B., Song, J., Yuan, H., Li, X., & Li, N. (2014). Air-sea CO_2 exchange process in the southern Yellow Sea in April of 2011, and June, July, October of 2012. *Continental Shelf Research*, 80, 8–19. https://doi.org/10.1016/j.csr.2014.02.001

Qu, B., Song, J., Yuan, H., Li, X., Li, N., & Duan, L. (2017). Comparison of carbonate parameters and air-sea CO_2 flux in the southern Yellow Sea and East China Sea during spring and summer of 2011. *Journal of Oceanography*, 73(3), 365–382. https://doi.org/10.1007/s10872-016-0409-6

Qu, B., Song, J., Yuan, H., Li, X., Li, N., Duan, L., et al. (2015). Summer carbonate chemistry dynamics in the Southern Yellow Sea and the East China Sea: Regional variations and controls. *Continental Shelf Research*, 111, 250–261. https://doi.org/10.1016/j.csr.2015.08.017

Song, J., Qu, B., Li, X., Yuan, H., Li, N., & Duan, L. (2018). Carbon sinks/sources in the Yellow and East China Seas—Air-sea interface exchange, dissolution in seawater, and burial in sediments. *Science China Earth Sciences*, 61(11), 1583-1593. https://doi.org/10.1007/s11430-017-9213-6

Su, J., (1998). Circulation dynamics of the China Seas north of 18°N. The sea, 11, 483-505.

Takahashi, T., Olafsson, J., Goddard, J. G., Chipman, D. W., & Sutherland, S. C. (1993). Seasonal variation of CO_2 and nutrients in the high-latitude surface oceans: A comparative study. *Global Biogeochemical Cycles*, 7(4), 843–878. https://doi.org/10.1029/93GB02263

Takahashi, T., Sutherland, S. C., Sweeney, C., Poisson, A., Metzl, N., Tilbrook, B., et al. (2002). Global sea-air CO_2 flux based on climatological surface ocean pCO_2, and seasonal biological and temperature effects. *Deep Sea Research Part II: Topical Studies in Oceanography*, 49(9–10), 1601–1622. https://doi.org/10.1016/S0967-0645(02)00003-6

Takahashi, T., Sutherland, S. C., Wanninkhof, R., Sweeney, C., Feely, R. A., Chipman, D. W., et al. (2009). Climatological mean and decadal change in surface ocean pCO_2, and net sea-air CO_2 flux over the global oceans. *Deep Sea Research Part II: Topical Studies in Oceanography*, 56(8–10), 554–577. https://doi.org/10.1016/j.dsr2.2008.12.009

Thomas, H., Bozec, Y., de Baar, H. J., Borges, A., & Schiettecatte, L. S. (2005). Controls of the surface water partial pressure of CO_2 in the North Sea. *Biogeosciences*, 2(4), 323–334. https://doi.org/10.5194/bg-2-323-2005

Tseng, C. M., Wong, G. T. F., Chou, W. C., Lee, B. S., Sheu, D. D., & Liu, K. K. (2007). Temporal variations in the carbonate system in the upper layer at the SEATS station. *Deep Sea Research Part II: Topical Studies in Oceanography*, 54(14–15), 1448–1468. https://doi.org/10.1016/j.dsr2.2007.05.003

Tsunogai, S., Watanabe, S., & Sato, T. (1999). Is there a “continental shelf pump” for the absorption of atmospheric CO_2?. *Tellus B: Chemical and Physical Meteorology*, 51(3), 701–712. https://doi.org/10.3402/tellusb.v51i3.16468

Van Alstyne, K. L., Nelson, T. A., & Ridgway, R. L. (2015). Environmental chemistry and chemical ecology of "green tide" seaweed blooms. *Integrative and comparative biology*, 55(3), 518–532. https://doi.org/10.1093/icb/icv035

Wang, B., Chen, J. F., Jin, H. Y., Li, H. L., Liu, X. Z., Zhuang, Y. P., et al. (2011). Preliminary study on the dissolved inorganic carbon system and its response mechanism in Changjiang River Estuary and its adjacent sea areas in summer. *Journal of Marine Science*, 29, 63–70. (In Chinese with English abstract)

Wang, S. L., Chen, C. T. A., Hong, G. H., & Chung, C. S. (2000). Carbon dioxide and related parameters in the East China Sea. *Continental Shelf Research*, 20(4–5), 525–544. https://doi.org/10.1016/S0278-4343(99)00084-9

Wang, X. H., Qiao, F., Lu, J., & Gong, F. (2011). The turbidity maxima of the northern Jiangsu shoal-water in the Yellow Sea, China. *Estuarine, Coastal and Shelf Science*, 93(3), 202–211. https://doi.org/10.1016/j.ecss.2010.10.020

Wang, B., & Wang, X. (2007). Chemical hydrography of coastal upwelling in the East China Sea. *Chinese Journal of Oceanology and Limnology*, 25(1), 16–26. https://doi.org/10.1007/s00343-007-0016-x

Wanninkhof, R. (2014). Relationship between wind speed and gas exchange over the ocean revisited. *Limnology and Oceanography: Methods*, 12(6), 351–362. https://doi.org/10.4319/lom.2014.12.351

Weiss, R. F. (1974). Carbon dioxide in water and seawater: the solubility of a non-ideal gas. *Marine chemistry*, 2(3), 203–215. https://doi.org/10.1016/0304-4203(74)90015-2

Weiss, R. F., & Price, B. A. (1980). Nitrous oxide solubility in water and seawater. *Marine chemistry*, 8(4), 347–359. https://doi.org/10.1016/0304-4203(80)90024-9

Wu, H., Shen, J., Zhu, J., Zhang, J., & Li, L. (2014). Characteristics of the Changjiang plume and its extension along the Jiangsu Coast. *Continental Shelf Research*, 76, 108–123.

Xu, X., Zang, K., Huo, C., Zheng, N., Zhao, H., Wang, J., & Sun, B. (2016). Aragonite saturation state and dynamic mechanism in the southern Yellow Sea, China. *Marine pollution bulletin*, 109(1), 142–150. https://doi.org/10.1016/j.marpolbul.2016.06.009

Xue, L., Zhang, L., Cai, W. J., & Jiang, L. Q. (2011). Air-sea CO_2 fluxes in the southern Yellow Sea: An examination of the continental shelf pump hypothesis. *Continental Shelf Research*, 31(18), 1904–1914. https://doi.org/10.1016/j.csr.2011.09.002

Zhai, W. D., Chen, J. F., Jin, H. Y., Li, H. L., Liu, J. W., He, X. Q., & Bai, Y. (2014). Spring carbonate chemistry dynamics of surface waters in the northern East China Sea: Water mixing, biological uptake of CO_2, and chemical buffering capacity. *Journal of Geophysical Research: Oceans*, 119(9), 5638–5653. https://doi.org/10.1002/2014JC009856

Zhai, W. D., & Dai, M. H. (2009). On the seasonal variation of air-sea CO_2 fluxes in the outer Changjiang (Yangtze River) Estuary, East China Sea. Marine Chemistry, 117(1–4), 2–10. https://doi.org/10.1016/j.marchem.2009.02.008

Zhai, W. D., Dai, M. H., & Guo, X. H. (2007). Carbonate system and CO_2 degassing fluxes in the inner estuary of Changjiang (Yangtze) River, China. *Marine chemistry*, 107(3), 342–356. https://doi.org/10.1016/j.marchem.2007.02.011

Zhang, J., Huang, W. W., Liu, M. G., & Zhou, Q. (1990). Drainage basin weathering and major element transport of two large Chinese rivers (Huanghe and Changjiang). *Journal of Geophysical Research: Oceans*, 95(C8), 13277–13288. https://doi.org/10.1029/JC095iC08p13277

Zhang, L., Xue, L., Song, M., & Jiang, C. (2010). Distribution of the surface partial pressure of CO_2 in the southern Yellow Sea and its controls. *Continental Shelf Research*, 30(3–4), 293–304. https://doi.org/10.1016/j.csr.2009.11.009

AGU PUBLICATIONS

Journal of Geophysical Research: Oceans

Supporting Information for

Spatio-temporal variability of the carbonate system and air-sea CO_2 fluxes in the South Yellow Sea and East China Sea during the warm seasons

Xue Deng[1,2], Gui-Ling Zhang[1,2], Ming Xin[2,3], Chun-Ying Liu[1,2,*], Wei-Jun Cai[4]

[1] Key Laboratory of Marine Chemistry Theory and Technology, Ministry of Education, Qingdao 266100, PR China

[2] Laboratory for Marine Ecology and Environmental Science, Qingdao National Laboratory for Marine Science and Technology, Qingdao 266071, PR China

[3] Key Laboratory for Marine Bioactive Substances and Modern Analytical Technology, the First Institute of Oceanography, Ministry of Natural Resources, Qingdao 266061, PR China

[4] School of Marine Science and Policy, University of Delaware, Newark, DE 19716, United States

*Corresponding author: roseliu@ouc.edu.cn

Contents of this file

Introduction

This file shows the vertical distributions of temperature and salinity in transect B in the SYS in spring cruise.

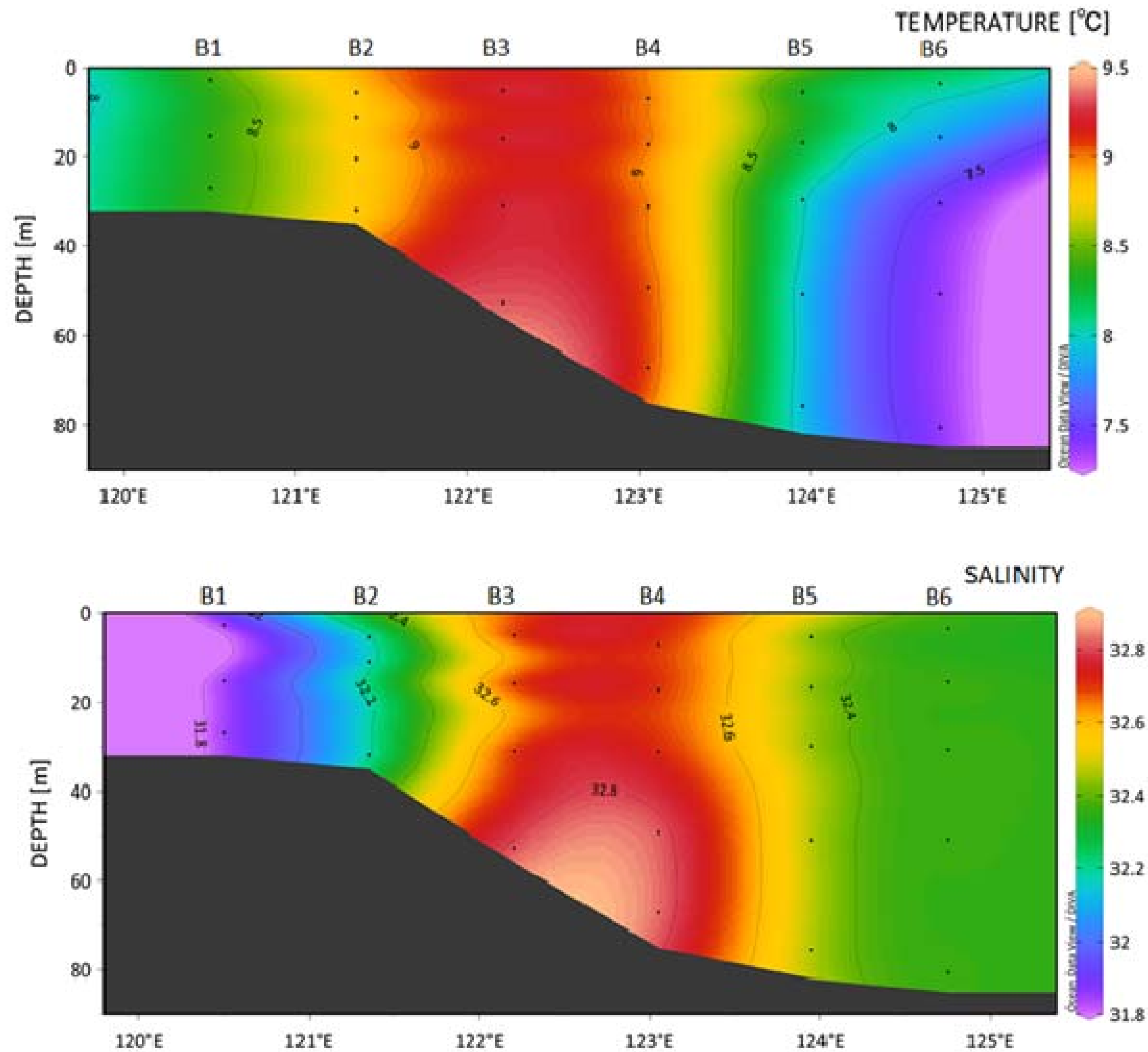

Figure S1. Vertical distributions of temperature and salinity along transect B in spring.